

Date: 1/5/15

EIC Detector R&D Progress Report

Project ID: eRD1

Project Name: EIC Calorimeter Development

Period Reported: from 7/1/14 to 12/31/14

Project Leaders: H.Huang and C.Woody

Contact Person: C.Woody

Collaborators

***S.Boose, J.Haggerty, J.Huang, E.Kistenev, E.Mannel, C.Pinkenberg,
S. Stoll and C. Woody***
(PHENIX Group, Physics Department)

E. Aschenauer, S. Fazio, A. Kiselev
(Spin and EIC Group, Physics Department)

Y. Fisyak
(STAR Group, Physics Department)
Brookhaven National Laboratory

F. Yang, L. Zhang and R-Y. Zhu
California Institute of Technology

T. Horn
The Catholic University of America and
Thomas Jefferson National Accelerator Facility

W. Jacobs, G. Visser and S. Wissink
Indiana University

C. Munoz-Camacho
IPN Orsay, France

S. Heppelmann
Pennsylvania State University

C. Gagliardi and M.M. Mondal
Texas A&M University

L. Dunkelberger, H.Z. Huang, K. Landry, Y. Pan, S. Trentalange, O. Tsai
University of California at Los Angeles

Y. Zhang, H. Chen, C. Li and Z. Tang
University of Science and Technology of China

H. Mkrtychyan
Yerevan Physics Institute

Abstract

This report describes the progress of the EIC Calorimeter R&D Consortium for the period 7/1/14 – 12/31/14. The effort was divided into four main areas: 1) Development of an electromagnetic calorimeter based on a matrix of tungsten powder and epoxy with embedded scintillating fibers (W/SciFi); 2) The study of radiation damage in silicon photomultipliers (SiPMs) and how it would affect their use in an EIC detector; 3) Development of scintillating crystals for an electromagnetic calorimeter in the forward electron going direction at EIC; 4) Simulations on calorimetry and related detector systems for an overall EIC detector. Since the last report to the Committee, the BNL PHENIX team has joined the UCLA team in developing the W/SciFi calorimeter. This was motivated by the adoption of this technology for the central electromagnetic barrel calorimeter for the upgrade to the PHENIX experiment (sPHENIX) which would eventually lead to a detector for eRHIC. The main efforts on developing this technology has been to try and improve the light collection uniformity within the modules, develop a high resolution version of the modules that could achieve an energy resolution $\sim 6\%/\sqrt{E}$, develop a cost effective mass production method for producing the quantity of modules that would be needed for a full scale barrel calorimeter, and to try and develop a method of producing fully projective modules. The study of radiation damage in SiPMs focused on neutron induced damage and investigating ways to deal with the large increase in dark current that is produced by irradiation. The effort on scintillating crystals consisted of two main parts. One was developing a viable source of PbWO_4 crystals for use in a high resolution electromagnetic calorimeter in the forward going electron direction at EIC, and the second was the continued investigation of BSO crystals as a low cost alternative to PbWO_4 . The effort on simulations supported all of our other efforts in providing valuable guidance as to the requirements and expected performance of the various detectors. Many of these simulation results are presented in the newly released eRHIC Design Study that is now available on the web (<http://arxiv.org/pdf/1409.1633.pdf>).

Sub Project: Progress on EIC Calorimeter R&D by UCLA/BNL/IU/PSU/TAMU Team
Project Leader: H. Huang

Overview

Over the past six months the main goals of our group's collaboration were:

- To continue development of a compact light collection scheme for W powder ScFi calorimeters. This was a follow up of a test run at FNAL in March of 2014.
- Investigate options for a high resolution electromagnetic calorimeter in the outgoing lepton direction at EIC. This was a follow up of a global optimization of the EIC detector.
- Investigate options of 'industrialization' of production of W powder ScFi type calorimeters.

We worked closely with the BNL EIC group and the BNL PHENIX group during the past six months to advance these goals. We plan to carry out a test run at FNAL with the re-worked forward EM prototype and a new high resolution EM prototype in late spring of 2015. A request for a two week time slot has been submitted to FNAL.

Past

What was planned for this period?

- Study ways to improve the uniformity of light collection of the W-SciFi modules, and hence their energy resolution and uniformity of response, by introducing an optical filter between the fibers and the SiPM readout
- Design a high resolution W-SciFi module ($\sim 6\%/\sqrt{E}$) which could be used in the forward going lepton direction at EIC
- Investigate ways of industrializing the fabrication of W-SciFi modules for large scale calorimetry

What was achieved?

1. Improving uniformity of light collection:

The forward calorimeter prototype tested at FNAL in 2014 was reworked in order to study ways of improving its light collection uniformity. The front face of the calorimeter modules measured in the test beam were machined and polished to allow for high resolution scans with a UV LED that was used to excite scintillation fibers at the front face of the prototype. Exactly the same readout electronics used in the test beam was used to read out this prototype for the scans. Summer students performed measurements on all four super modules of the prototype. An example of one of these scans is shown in Figure 1, where X and Y are in (mm) and center of the super block (the corner between four individual towers) is at the center of the figure. The drop in signal of about 10% in the center of the superblock is related to the non-uniformity of light collection with the compact light guides and SiPMs that were used in the prototype.

The current plan is to introduce a filter between scintillation fibers and light guides to flatten the response shown on Figure 1. We are considering two options. Both will require an additional flat acrylic plate approximately 5 mm thick, which will be glued to the end of the W/ScFi blocks. The filter can be printed directly to this acrylic plate (option 1) or the filter can be a thin metallic mesh with the desired density of the holes which will be glued to this plate (option 2). Light guides similar to one used in the test beam run will then be glued to this intermediate acrylic plate with the filter. Both options have pros and cons, which we are considering at present. The total reduction of light by

the filter will be about 20%. However, this is not a problem, since we have about factor of 1.5 more lights in our current prototype than is needed in order that photostatistics do not contribute significantly to the energy resolution. Both options are suitable for industrialization. The plan is to produce light guides for 16 channels at once with an injection molding technique in the future, as well as a filter plate, irrespective of whether it will be a mesh or will be printed. At present, the backside of the forward prototype was machined (after removing all light guides) and new sets of light guides, produced with exact the same geometry but with the filter, will be finalized early next year. We will then repeat the scans with the re-worked light collection scheme before the next test beam run.

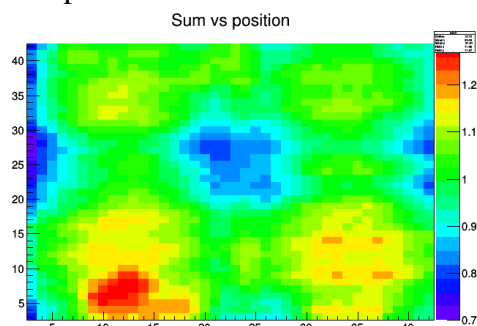


Figure-1. Normalized response of the forward EM prototype when scintillation fibers were excited with UV LED at the front surface of the prototype.

2. High resolution W-SciFi modules

The latest EM prototypes tested at FNAL had an energy resolution at about 10% at 1 GeV. For the dedicated EIC detector, with a 3T magnetic field and high resolution MAPS tracking detectors in the forward electron going direction, an energy $\sim 6\%/\sqrt{E}$ may be sufficient to identify the outgoing electron and achieve good electron/hadron separation (see Appendix to this report on simulations). To improve the energy resolution by a factor of two over what was measured in the test beam (which is a substantial increase in performance) will require increasing the sampling fraction as well as the sampling frequency at the same time. However, there are some pure technological limits, which may be a problem. To increase the sampling fraction, we investigated the possibility of making the absorber out of different types of metals. While many types of metals are available as a powder, the most suitable for our applications is Sn. It has high Z, available in the correct particle size, is non-abrasive, non-toxic, and is relatively non-expensive. The alternative can be Cu, but its lower Z makes it less attractive, although cost wise it is very cheap. Industrial methods of mixing of different powders are well developed. We produced a few samples of composite absorbers W/Cu, W/Sn (50%/50% by weight) as shown in Figure 2. Infusion of epoxy up to 7 cm depth can be made in about 15 minutes for 100 mesh powders. The density of W/Sn absorber shown in Figure 2 and is 7.4 g/cm^3 .

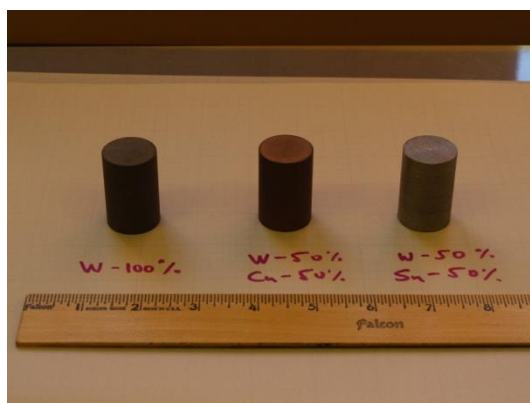


Figure-2. Samples of composite absorbers.

Several MC calculations for the EM calorimeter in the outgoing lepton direction built with such absorbers and different fiber sampling frequency and diameters are shown in Figure 3. The dilution of absorber with only the same fiber arrangement used in our previous prototypes will improve the energy resolution to about 8% at 1 GeV as shown in green in Figure 2. To get the desired 6% will require diminishing the diameter of the fibers from 0.47 mm to 0.4 mm and decreasing the spacing between them from 0.995 mm to 0.67 mm as shown in Figure 3 in magenta. This is our basic configuration for our first high-resolution prototype we will prepare for the test run in 2015.

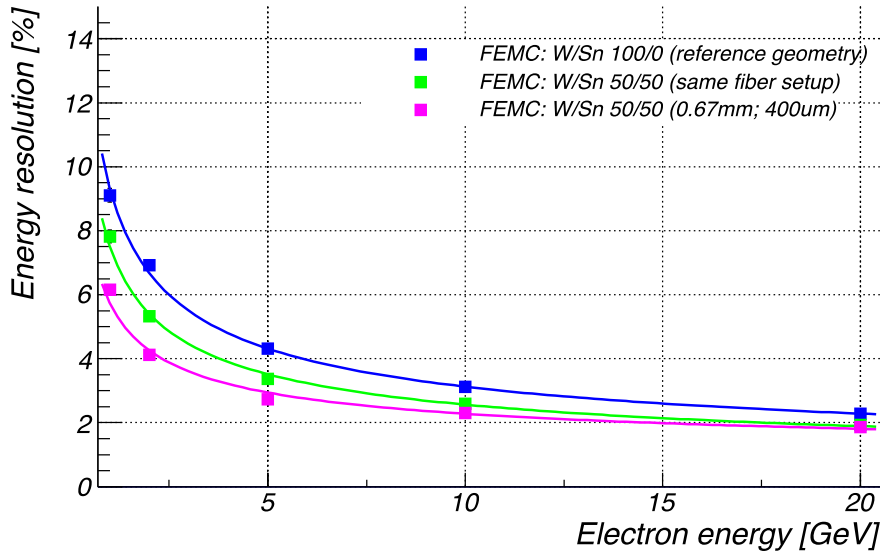


Figure-3. Energy resolutions of FEMCs with different compositions of absorbers and fibers.

There are a few concerns at the moment regarding this technology with this basic geometry. The dimensions of the super-blocks increased due to the lower density of the material. They are 5 cm x 5 cm x 25 cm. The super block will hold about 6000 fibers, which is about a factor of two more than that in our previous prototypes. We will be using thinner meshes to allow for the increased sampling frequency (which is at the limitation of the etching process), and we will use longer and thinner scintillation fibers to fill the meshes. The concern is how much more difficult it will be to create such fiber assemblies compared to our previous prototypes. We have built spacordion prototypes with even thinner fibers (0.33 mm in diameter) but they were only 17 cm long and had a spacing of 1 mm. Without trying the assembly procedure with real components it is difficult to predict how well our process of making fiber assemblies will work. We have ordered the required fibers from KURARY and expect to carry out the first test with them at the end of January 2015. The instrumental effects (such as attenuation length, potential variation of local density in the super-modules) may also limit the resolution. At present, the MC model only includes a few of them, which are educated guesses at this time due to lack of real bench test measurements.

3. Industrialization of W-SciFi module production

The method and plan for mass production of EM modules remain an open issue. A fully industrialized method is possible by transferring the technology developed at UCLA to industry. However, it is probably not the most cost-effective method. The simple task of arranging the fibers for the EM modules could be carried out by any university group with assemblies being made by undergraduate students. The investment into infrastructure to perform this task is minimal and several groups can easily do such production in parallel. Filling with powder and infusion of epoxy into these fiber assemblies is better done by industry or at a single production facility using teams of trained technicians.

We have just started to transfer the technology to construct W/SciFi modules to Tungsten Heavy Powder (THP), which is a private manufacturing company in San Diego that supplies the tungsten powder for the modules, and to the BNL PHENIX group and to UIUC PHENIX group. Personnel from THP visited UCLA twice in the past six months, as shown Figure 4. The THP team went thru the whole production procedure and discussed all technological steps which require optimizations for mass production. At present, THP wants to adopt their standard method using pre-mixed powder and epoxy and centrifugal injection of this mixture into fiber assemblies provided by UCLA. In December, groups from BNL and UIUC visited UCLA to learn the technique to build EM modules as well, which is related to the plan to use these types of modules in sPHENIX. As with THP, we went through the whole cycle of production, tooling etc. The current plan is that these two groups will independently produce and test a few prototypes in early 2015, first following the UCLA technique, and then developing a new construction technique for fully projective towers. Also in December, the groups from BNL, UCLA, UIUC visited THP to look at their production capabilities and discussed our R&D plan for 2015. There are also other options to arrange for mass production in one of the Chinese universities or in one of the Russian institutions in future which are also under consideration. These options will not be pursued until we know better what THP will be able to deliver in early 2015. We expect that with the strong focus on the development of detector construction techniques by several groups in 2015 we will be able to achieve significant improvements on the construction technique that is suitable for mass production of EMC modules appropriate for STAR, sPHENIX and EIC applications.



Figure 4. THP personnel at UCLA

What was not achieved, why not, and what will be done to correct?

1. Preliminary studies were done on how to improve the light collection uniformity of the W/SciFi modules using an optical filter. These studies will be completed and modifications to an array of modules will be implemented during the next period.
2. Preliminary studies on low density absorbers were carried out and final modules with a low density absorber, smaller fiber diameter and decreased fiber spacing will be built and tested during the next period.
3. Initial meetings were held at UCLA with THP and members of the BNL and UIUC physics groups to learn the technique and hands-on experience for building W/SciFi modules and discuss future plans for mass production of modules and for making fully projective modules. Initial modules will be produced by each of these groups in early 2015.

Future

What is planned for the next funding cycle and beyond? How, if at all, is this planning different from the original plan?

1. Complete the studies on how to improve the light collection uniformity within a single tower module using an optical filter and implement this improvement on an array of towers.
2. Construct an array of modules consisting of a low density absorber (Sn) with smaller fiber diameter (0.4 mm) and smaller fiber to fiber spacing (0.67 mm).
3. Test the modules constructed in 1 and 2 above in a test beam at Fermilab.
4. Build and test W/Sci modules at THP, BNL and UIUC. The effort with the THP will be focused on improving the efficiency of production and lowering the cost in order to develop a process for future mass production.

What are the critical issues?

1. Demonstrate improvement in the uniformity of light collection using an optical filter and its improvement in the energy resolution and uniformity of response of the modules.
2. Demonstrate that it is possible to achieve an energy resolution $\sim 6\%/\sqrt{E}$ for a spacial type module using a low density absorber with smaller fiber diameter and a smaller fiber to fiber spacing.
3. Transfer the technology for building W/SciFi modules to other groups and develop cost effective mass production techniques for constructing modules.

Additional information:

We currently have sufficient funds to construct the prototype modules and carry out a beam test run at FNAL in spring 2015. We plan to request additional funds at the July R&D review meeting in 2015 at the level of \$130k. This would include \$50K of R&D funds that would be needed for effort at THP for the development of mass produced W/SciFi modules. We also expect that some PHENIX R&D funds would also support this effort. Further details of the R&D scope will be developed after the analysis of the test run data.

Sub Project: Progress on EIC Calorimeter R&D at BNL

Project Leader: C. Woody

Overview

As stated in our last report from June 2014, the BNL group has abandoned the concept of developing an optical accordion tungsten plate calorimeter for EIC. This decision was based on the difficulty in manufacturing the accordion plates and adhering to the necessary tolerances within a reasonable cost, as well as the poor performance in terms of energy resolution that was measured with a flat tungsten plate prototype calorimeter in the test beam in February of 2014. All of this was learned through this EIC R&D program, which has provided valuable guidance for the future. We have therefore consolidated our effort with the UCLA group to develop the tungsten scintillating fiber spacial design and are working with them to further enhance this design and to develop methods of mass production for future large scale calorimetry. We are also increasing our own effort on studying radiation damage in silicon photomultipliers. This is based on the fact that radiation damage in SiPMs will be a major issue for any detector using these devices at RHIC or EIC, and a detailed investigation as to how the effects of radiation damage in SiPMs will affect their operation in future detectors at EIC is warranted.

Past

What was planned for this period?

Our main focus was to redirect our effort onto the development of the tungsten fiber spacial design that was initiated by UCLA. We have now adopted this as our baseline design for the EMCAL for sPHENIX, which would also serve as the basis for a future eRHIC detector. Our goal for this period was to better familiarize ourselves with the design and construction of the W/SciFi modules, learn how to fabricate modules of our own, explore ways of constructing fully tapered modules, and study the performance of the W/SciFi spacial in sPHENIX using Monte Carlo simulations.

We also planned a series of radiation damage studies on different types of SiPMs from different manufacturers. These included neutron irradiations using a neutron generator at the Brookhaven Solid State Radiation Facility, tests at the Los Alamos Neutron Science Center (LANSCE), and tests at the Indiana Cyclotron Facility.

What was achieved?

We have acquired drawings and specifications for construction of W/SciFi modules similar to the ones that have been constructed at UCLA. A group of us (C.Woody, S.Stoll and J.Huang from BNL, and A. Sickles and one of her technicians from the UIUC) visited UCLA in early December. We participated in the construction of a two tower module while we were there and discussed various improvements to the construction procedure with O.Tsai. We also discussed various possibilities for constructing fully tapered modules (i.e., trapezoidal shaped modules that are tapered by different amounts in two orthogonal directions, as opposed to the current design, which is projective in only one dimension). This would allow construction of a fully projective central barrel calorimeter, which would have many advantages in terms of particle ID. We all then visited THP, accompanied by O.Tsai and H.Huang from UCLA, where we toured their facility and discussed alternative ways of constructing the modules that would be more suitable for mass production. This would involve filling preformed fiber assemblies (fibers stacked between arrays of meshes) and then filling these assemblies with a mixture of tungsten powder and epoxy. The filled assemblies would

then be centrifuged to achieve their final density. This procedure would allow multiple modules to be formed simultaneously and would greatly reduce the number of steps in producing individual modules. We agreed that the next step forward would be to have THP construct a set of modules using this technique, which would then be evaluated by physicists. If successful, THP would then produce a set of 24 modules that would be tested in the test beam in order to perform a direct comparison with similar modules that were tested by the UCLA/BNL/TAMU/PSU team in February 2014.

We also began to investigate the possibility of producing doubly tapered modules. One idea is shown in Fig. 1. It would use two different screens with long slots that would allow the fibers to pass through and could be rotate independently in two orthogonal directions. Each screen would be set at a specific angle in order to achieve the desired taper in each direction. Once the double tapered fiber assemblies are in place, the procedure for fabricating the modules would remain the same.

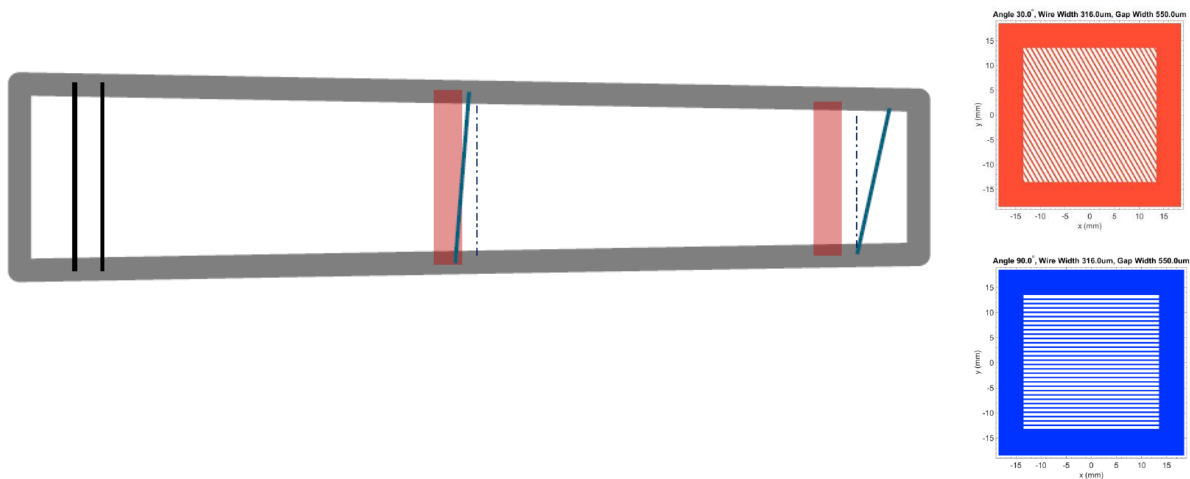


Figure 1: Possible method for producing modules with different tapers in two directions, resulting in a fully projective module.

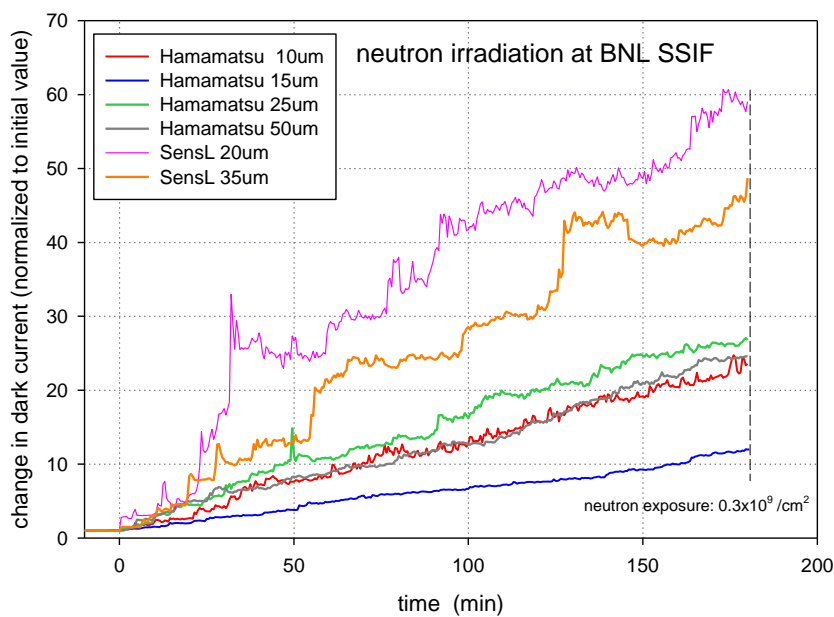


Figure 2: Relative change in dark current for various types of SiPMs from Hamamatsu and SensL for a neutron flux up to $0.3 \times 10^9 \text{ n/cm}^2$.

We also carried out a number of studies on radiation damage in SiPMs. These were mostly carried out at the BNL Solid State Radiation Facility, which has a D-T neutron generator capable of producing high fluxes of 14 MeV neutrons using a deuterium beam on a tritium target. We obtained samples of SiPMs from a number of manufacturers and compared their performance for neutron fluxes up to $0.3 \times 10^9 \text{ n/cm}^2$. Tests were also performed on devices at LANSCE with $>10 \text{ MeV}$ neutrons up to a flux of $7.2 \times 10^{10} \text{ n/cm}^2$.

Figure 2 gives an example of some of the results obtained. We observed a significant increase in dark current for each of the SiPMs tested for a neutron exposure of $0.3 \times 10^9 \text{ n/cm}^2$. The relative changes were in the range of 10-60, while the initial currents were in the range of 10's-100's of nA. Therefore, the resulting currents reached levels of several μA . For a device that was exposed to $8.5 \times 10^{10} \text{ n/cm}^2$ at LANSCE, the dark current increased to 1 mA.

Figure 3 shows the change in the single photoelectron spectrum for a $25 \mu\text{m}$ Hamamatsu device that was exposed to dose of $0.3 \times 10^9 \text{ n/cm}^2$. It is clear that the single photoelectron peaks are no longer resolved due to the high noise and dark count rate.

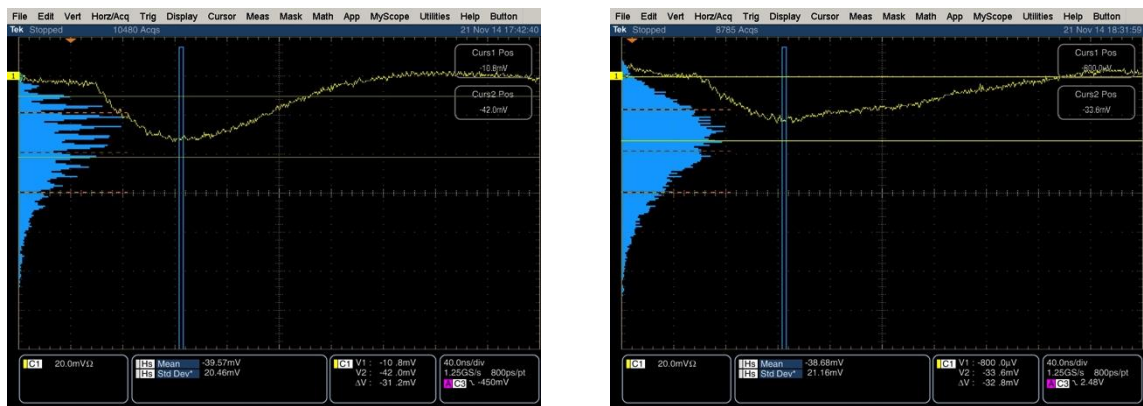


Figure 3: Single photoelectron spectrum for a Hamamatsu S12572-025P before and after exposure to a neutron flux of $0.3 \times 10^9 \text{ n/cm}^2$.

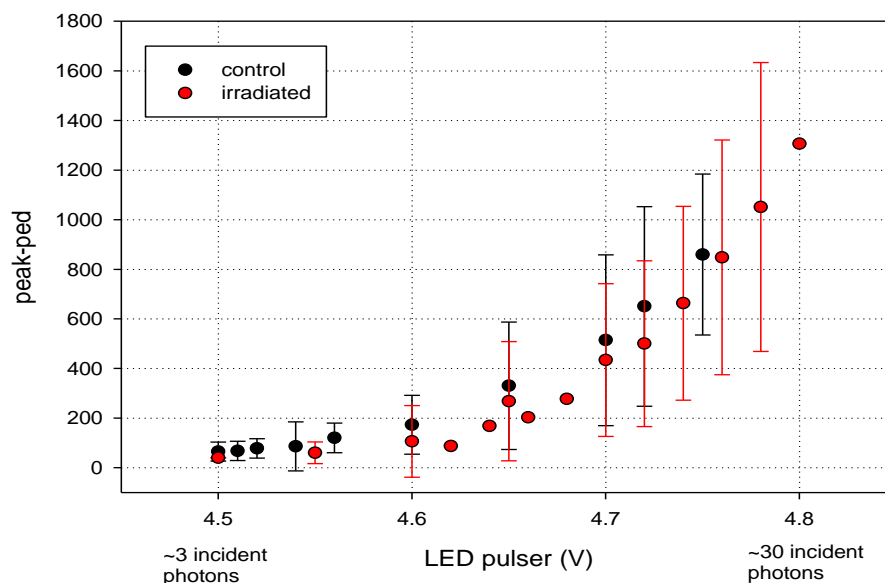


Figure 4: Signals measured near the noise level in a Hamamatsu S12572-025P SiPM before and after exposure to a neutron flux of $0.3 \times 10^9 \text{ n/cm}^2$.

The consequences radiation exposure in terms of using these devices for calorimetry at EIC is not fully understood. The most apparent effect of the exposure is that the single photoelectron dark count rate increases dramatically. However, it does not appear that the normal operation of the device is otherwise adversely affected. We measured the operation of one of the 25 μm pixel Hamamatsu SiPMs after exposure with a LED pulser for relatively low light levels which produced signals close to the noise. Figure 4 gives the results of this measurement and shows that it is still possible to measure very small signals, which are close to the noise even with the high noise rate.

It should also be noted that in Fig. 2, the 15 μm pixel Hamamatsu device showed the least increase in dark current relative to the other devices. Tests with the same Hamamatsu device by the CMS experiment have shown similar results. Having a smaller pixel size does tend to decrease the effect of the radiation induced noise, since a smaller area of the device is affected by any given localized damage. However, it is not clear why the 10 μm pixel Hamamatsu device did not perform better in this case.

Another effect of the increased dark current is that the gain of the device may change due to the voltage drop produced by the dark current across the quenching resistor or any external current limiting resistor. The increased current will increase the voltage drop across this resistor, which would decrease the gain of the device and also cause additional ohmic heating. These effects can in principle be compensated for with external electronics, but the ability to do so must be designed into the voltage control and temperature stabilization system.

What was not achieved, why not, and what will be done to correct?

We accomplished essentially all of our goals for this period. We did not begin to actually construct W/SciFi modules at BNL, but all materials necessary to do so are either in hand or on order.

We carried out a numerous radiation damage tests on SiPMs with neutrons and now have a large collection of data to analyze. We did not irradiate samples at the Indiana Cyclotron Facility due to a change in their schedule, but we hope to be able to carry out those measurements early next year.

Future

What is planned for the next funding cycle and beyond? How, if at all, is this planning different from the original plan?

We are currently working on fabricating the necessary molds to construct our own W/SciFi modules at BNL and we should be able to begin constructing 1D projective modules in early January. We have also identified a supplier of the new screens that will be used to try and construct 2D projective modules and will order those materials in early January as well. After acquiring experience with building 1D projective modules, we will then attempt to build 2D projective modules using various techniques.

We are expecting to receive the first modules produced at THP by early February. We will test and evaluate these modules in terms of their mechanical properties and tolerances, density and uniformity of the fibers within the matrix. We will also check for any damage to the fibers that may have occurred due to the new manufacturing process that THP is developing. If the first modules are satisfactory, we will ask them to construct a 4x6 matrix of modules using the same manufacturing method which we will then test in the test beam to compare with similar modules that were built and tested by UCLA in 2014. We will work with both UCLA and UIUC on the evaluation and testing of these modules as well as in the beam test.

If our attempt to build fully 2D projective modules is successful, we will transfer this technology to THP and have them attempt to build a set of modules using their manufacturing technique.

The only difference in terms of their process should be that the fiber assemblies, and hence the molds that they use, will be of a slightly different shape.

We also plan to continue our studies on radiation damage in SiPMs. Based on our current measurements, the 15 μm Hamamatsu devices seem to have the least effect from neutron irradiation compared to other devices tested. We will continue to study these devices as well as those from other manufacturers. We will also continue to study how to use radiation-damaged devices for actual calorimetry measurements. This may involve cooling the devices and building new electronics that will compensate for changes in gain and temperature caused by radiation.

What are the critical issues?

Developing an efficient, cost effective mass production method for constructing W/SciFi calorimeter modules that would be used for a barrel EMCAL at EIC.

Develop a simple, cost efficient procedure for producing fully 2D tapered W/SciFi modules for a central barrel calorimeter. This is mainly a requirement for PHENIX, since its electromagnetic calorimeter must also be used for heavy ion collisions, but since the same calorimeter would be used in an upgraded PHENIX experiment for EIC, it is important that this issue be addressed when the calorimeter is constructed.

Understanding the effects of radiation damage in SiPMs and how they affect their use for calorimetry at EIC. It is clear that neutron radiation causes a large increase in dark current for all devices. However, some devices perform better than others, and we need to identify which devices are best suited for use at EIC. We must also find ways of dealing with the high noise and dark current in radiation damaged devices. This could involve cooling the devices in situ, as well as developing electronics that can compensate for the changes in gain that will result due to the increased dark current, along with better temperature stabilization that will result from the heat which is generated.

Develop a better estimate of the actual radiation levels, both from neutrons as well as from ionizing radiation, that various detectors will be exposed to at EIC. It is not an easy task to make such an estimate, since it involves various types of machine related backgrounds, as well as a detailed model of the detectors and the experimental halls. However, at the present time, certain estimates of radiation levels in the RHC experimental halls can be used.

Additional information:

We expect to request additional funds at the level of approximately \$50K in FY16. This will involve \$15K for supplies and materials for building W/SciFi modules, \$15K for radiation damage studies and \$3K for travel and support of test beam activities. The total direct cost for these items is \$33K and the total funding request will be \$50K including a factor of 1.5 for overhead.

Sub Project: Crystal Calorimeter Development for EIC based on PbWO₄

Project Leader: T. Horn

Overview

An important requirement for the EIC endcap electromagnetic calorimeter is high-resolution in the electron going direction in order to measure the energy of the scattered electron with high precision. The calorimeter should provide angular resolution to at least 1 degree to distinguish between clusters, have an energy resolution $\sim \text{few } \%/ \sqrt{E}$ for measurements of the cluster energy, and withstand radiation to at least 1 degree with respect to the beam line. Crystal calorimeters have been used in nuclear and high energy physics for their high resolution and detection efficiency and thus would be the preferable solution for the future EIC. In particular, a solution based on PbWO₄ would be optimal due to its small Moliere radius and radiation hardness. PbWO₄ has been used for existing calorimeters (CMS, JLab Hall B) and high quality crystals are being considered to be used in several new electromagnetic calorimeter projects around the world (PANDA, JLab 12 GeV). The critical aspect for crystal quality, and thus resolution, is the combination of high light output and radiation hardness, which depend strongly on the manufacturing process. During the CMS ECAL and early PANDA EMC construction, two manufacturers, BTCP and SIC, using different crystal growth methods were available. Basically all high quality crystals have been produced at BTCP using the Czochralski growing method, whereas SIC produces crystals using the Bridgman method. BTCP is now out of business, and the worldwide availability of high quality PbWO₄ production has changed dramatically. Recent studies of crystals from SIC, the remaining manufacturer of crystals, seem to indicate major problems maintaining good crystal quality. It is therefore not clear if crystals of the same quality as those produced by BTCP are in fact currently available. Based on this current situation, there is a clear need to develop an alternate supplier of PbWO₄ if it is to be used for a future EIC crystal calorimeter in parallel with the current efforts. The main goal addressed by the proposed R&D is to identify what would need to be done to be able to build a PbWO₄-based endcap calorimeter for the EIC exploring the limits of PbWO₄ quality. Such an R&D effort fits naturally into the global EIC calorimeter R&D program and could also have an impact on the worldwide PbWO₄-based electromagnetic calorimeter construction.

Past

What was planned for this period?

The main goals for this project in this time period were:

- Get started with setting up the infrastructure for crystal testing.
- Plan meetings for 2014/15 to exchange information on crystal testing.

What was achieved?

The Crystal Calorimeter Development for EIC based on PbWO₄ component of the EIC Calorimeter Consortium was submitted, presented, and recommended to be funded in full. In preparation for testing the crystal performance the university lab infrastructure at Orsay and CUA is being optimized for such tests. For example, the group at IPN-Orsay has started looking into the procurement of an optical spectrometer in order to measure transmittance of PbWO₄ samples onsite. Similar equipment as the one used by the PANDA Collaboration is envisioned and it will be setup in collaboration with the group at Giessen. Contacts have been initiated with the companies VARIAN and HITACHI in order to procure the equipment. In addition, IPN-Orsay will benefit from the infrastructure of the University of Paris-Sud. In particular, a recent 50 MeV electron accelerator is on campus and will be used to induce high radiation doses to crystals, measure their radiation hardness and test

different bleaching procedures. Contacts have been initiated in order to allocate some beam time for these tests once the setup to measure crystal transmittance is ready. We expect all infrastructure to be in place before the Spring EIC R&D meeting making possible crystal testing before the end of FY15.

To take full advantage of the expertise of the Giessen group (also building the EMC for PANDA), a number of meetings were arranged to exchange knowledge. Carlos Munoz-Camacho visited the facilities in Giessen and Rainer Novotny met with Carlos Munoz-Camacho, Hamlet Mkrtychyan, and Tanja Horn at JLab and provided feedback on the procedures for testing the crystal quality.

Procedures for PWO crystal characterization, irradiation, and optical and temperature recovery were developed and tested. As an example, to test the method for optical recovery a system was constructed and its efficiency is being tested at Jefferson Lab during the currently running DVCS experiment in Hall A. The expected radiation dose that the PWO crystals will be exposed to is on the order of a few krad/hour.

PWO crystal irradiation tests at higher radiation doses have been scheduled for 2015 at the Idaho Accelerator Facility, which provides doses of 3.6 kGy (360 krad in 20 minutes). Earlier measurements done by one of us on PbF2 crystals, which were also produced at SIC, showed that a few minutes of irradiation can produce large effects and large fluctuations in radiation hardness were observed (see Fig.1). The results of optical transmittance measurements were shown to correlate well with visual inspection.

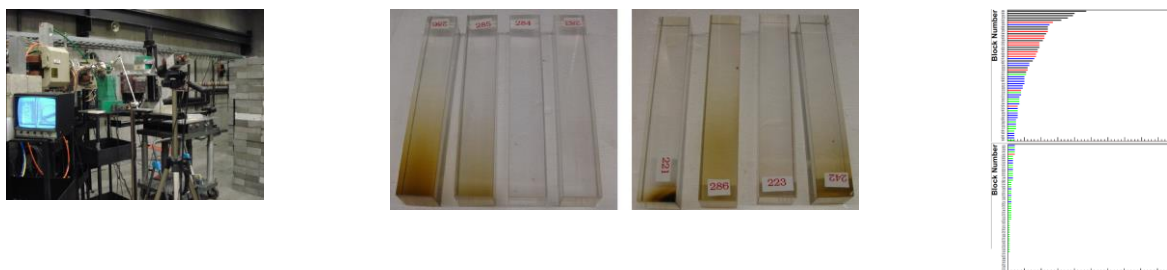


Figure 1: (left) the irradiation setup at the Idaho Accelerator Facility; (middle) a subset of eight PbF2 crystals (manufactured at SIC in 2009/10) showing very different response after irradiation for 20 minutes; (right) the difference of optical transmittance measurements before and after show large fluctuations in crystal response consistent with visual inspection.

Collaboration has been established with the JLab MEIC detector group to carry out calculations of the expected rates at the location of the calorimeter. Configurations are being explored with an inner high resolution crystal calorimeter and an outer calorimeter.

To give a first idea of the Crytur crystal performance we present here the results from a study of the first (small size) PWO crystals grown in collaboration with the Institute of Physics in Prague.



Figure 2: (left) La+Y doped PbWO4 crystal grown in N2+0.1%O2 atmosphere, (right) Sketch of the PbWO4 crystal cut.

Single crystals of approximate diameter 13.5 mm and length 32 mm, see Fig. 2 (left), were grown using the Czochralski technique (outer diameter of the platinum crucible was 4 cm, height 4 cm, thickness of the wall and of the bottom 5 mm; rate of growth of crystals was 5 mm/h, rate of rotation 50 rpm.). Except for the first crystal the material was remixed and sintered in one step at 500-835°C (500°C/1h-(695°C-735°C)/8h-835°C/6h), at which operation the material lost its surplus oxygen. After melting the melt was kept at approximately the melting temperature for about 20 hours before the crystallization. The crystals were cut into plates 1 mm thick and cylinders 10 mm thick, see sketch in Fig. 2 (right), and their faces were polished up to optical quality. These optical elements are noted by alphabet characters starting from “a” at the crystal seed side and proceeded along the crystal towards its end. Absorption and radioluminescence (X-ray excitation, 40 kV, 15 mA) spectra were measured at the plates. Absorption spectra before and after gamma ray irradiation (1.17 and 1.33 MeV γ -ray lines of ^{60}Co active source, 800 Gy dose delivered in approx. 15 hours) were measured at cylinders and the induced absorption coefficient spectra were calculated. Absorption spectra were measured with a spectrometer Shimadzu 3101PC and radioluminescence spectra were measured with a custom made 5000M model spectrofluorometer Horiba Jobin Yvon.

The following crystals were grown in this R&D phase:

1. Undoped PbWO_4 , denoted as PW-1T: plate 1Tb, cylinder 1Tc, plate 1Td. Grown under air atmosphere.
2. Y-doped PbWO_4 (50 at. ppm in the melt), PW-2T: plate 2Ta, cylinder 2Tb (calculated 42 ppm of Y in the sample considering segregation coefficient 0.8), plate 2Tc, 2Td, cylinder 2Te (calc. 48-62 ppm of Y in the sample), plate 2Tf. Grown under air atmosphere.
3. Y-doped PbWO_4 (100 at. ppm in the melt), photo in fig. 1b, PW-3T: plate T3a, cylinder T3b (calc. 82-87 ppm of Y in the sample), plate 3Tc, 3Td, cylinder 3Te (calc. 96-123 ppm of Y in the sample), plate 3Tf. Grown under air atmosphere.
4. Undoped PbWO_4 , PW-4, first part grown in dried nitrogen ($\text{N}_2 + 30\text{ppm O}_2$), then 120 liters of N_2 purified from O_2 was introduced in 36 minutes, concentration of O_2 decreased so to about 1 ppm (inner volume of the pulling machine is 30 liters). After about 30 minutes the crystal separated spontaneously from the melt and the experiment was stopped. The grown part of the crystal is strongly reduced and completely non-transparent. This reduction is probably connected with the introduction of oxygen-free atmosphere.
5. Undoped PbWO_4 , PW-5T: Plate 5Ta, cylinder 5Tb, plate 5Tc: grown under nitrogen + 0.1% oxygen atmosphere. Then 70 liters of dried N_2 were added and plate 5Td, cylinder 5Te and plate 5Tf were grown under nitrogen + 0.01% oxygen atmosphere.
6. La+Y (2:1) doped PbWO_4 , 1c, PW-6T: plate 6Ta, cylinder 6Tb (calc. average 207 ppm mol (La+Y) considering segregation coefficient of La 2.5), plate 6Tc, cylinder 6Td (av. 131 ppm mol La+Y), plate 6Te. Growth atmosphere nitrogen + 0.1% oxygen.
7. La+Y (2:1) doped PbWO_4 , PW-7T: plate 7Ta, cylinder 7Tb (calc. average 207 ppm mol La+Y), plate 7Tc, cylinder 7Td (av. 140 ppm mol La+Y), plate 7Te. Growth atmosphere was air.

The performance of the PW-6T crystal is comparable to the PANDA requirements regarding the absorption amplitude at 420 nm and the induced absorption coefficient amplitude at 420 nm ($\Delta k < 1.1 \text{ m}^{-1}$ at RT and integral dose of 30 Gy). We present the relevant absorption spectra of the PW-6T crystal in Figure 3 and Figure 4 below.

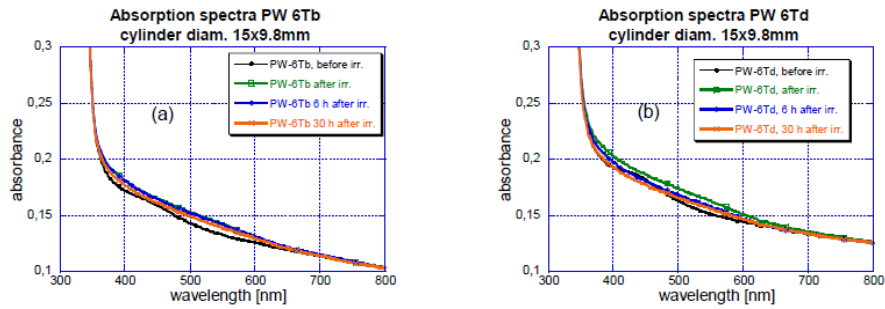


Figure 3: (left) Absorption spectra of PW 6Tb cylinder after ^{60}Co irradiation, (right) Absorption spectra of PW 6Td cylinder after ^{60}Co irradiation.

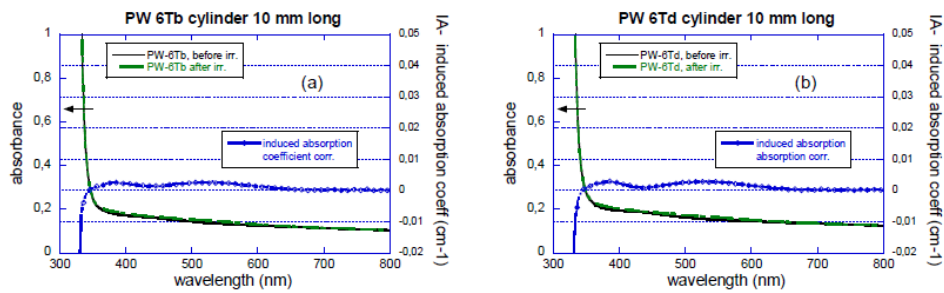


Figure 4: (left) Absorption spectra of PW 6Tb cylinder before and after irradiation and calculated induced absorption coefficient, (right) Absorption spectra of PW 6Td cylinder before and after ^{60}Co irradiation and the calculated induced absorption coefficient.

In general, the growth of the undoped PbWO_4 in air results in larger parasitic absorption over all the spectral region of scintillation emission (350-500 nm) and larger radiation damage. The growth of undoped PbWO_4 in completely oxygen-free atmosphere results in a non-transparent strongly reduced crystal. The growth of undoped PbWO_4 in $\text{N}_2 + 0.1\% \text{O}_2$ provides the crystal with better transmission characteristics and comparable radiation damage with respect to that grown in air atmosphere. The doping with sufficient amount of Y or La+Y (optimum seems to be within 100-200 at. ppm in the crystal) provides clearly better transmission characteristics especially below 400 nm (suppression of 350 nm parasitic absorption centre, and several times lower radiation damage at 420 nm). Such improvement is critical for good performance of PbWO_4 scintillators. The influence of the growth atmosphere seems to be less important (compare 6T and 7T crystal), but the combination of La+Y doping and $\text{N}_2+0.1\% \text{O}_2$ growth atmosphere in 6T provides the best set of characteristics. Y or La+Y doping reduces the total scintillation (radioluminescence) efficiency, but it is likely that this is due to suppression of slower components, which is in fact positive for fast response.

Crytur uses the Czochralsky technology to grow PbWO_4 crystals, which is identical to that used by BTCP. This two-stage growing procedure is well defined and additional know-how is available from experts from Minsk who are consultants in the process. The raw materials used were those used by BTCP and Crytur is in the position to acquire more of them when needed. To speed up the production of the first crystals the company elected to start the process with a half-closed oven. As discussed above studies at the Institute of Physics in Prague have shown that the best set of characteristics were achieved for doped crystals when the oxygen contribution is $<1\%$. These crystal growing conditions have been achieved at Crytur. Furthermore knowledge and expertise on machining and cutting PbWO_4 crystals are being transferred to Crytur giving the company a good starting point in crystal production.

What was not achieved, why not, and what will be done to correct?

There has been a delay in the Crytur full-size, i.e., 20-cm long, crystal procurement. The manufacturing process is very complex, but the company expects that on order 20 crystals will be available early in 2015.

Future

What is planned for the next funding cycle and beyond?

How, if at all, is this planning different from the original plan?

The planning for the next quarter will generally be as outlined in the proposal. We will, however, also try and work on providing answers to the question of the Advisory Committee to prepare an updated list of scintillating crystal specifications and their impact on the performance of an EIC detector. We hope to be able to report some results on this at the next meeting of the Advisory Committee. A more detailed explanation of how the crystal quality could affect the performance of the detector will also be provided. In general, electromagnetic calorimetry has two main functions: particle reconstruction, and particle identification (PID). The latter is important for discriminating single photons from, e.g., DVCS and two photons from π^0 decay, and electrons from pions. The reconstruction requirements is driven by the need to accurately reconstruct the four-momentum of scattered electrons at small angles, where the angular information is provided by the tracker, but the momentum (or energy) can come from either the tracker or the EM calorimeter. Since the calorimeter resolution follows the functional form $a/\sqrt{E}+b$, and the tracking resolution goes as $Ap + B/p + C$ (where B is due to multiple scattering), for high electron momenta there will always be a critical angle θ_0 , below which the EM calorimeter will, at high momenta in a solenoidal field, provide the stronger constraint. The tracking resolution for a dedicated EIC detector including a barrel silicon tracker and forward silicon trackers (forward GEM, barrel micromegas) is illustrated as a function of rapidity (angle) in Figure 5. At large absolute values of η (both forward and backward) the tracking resolution is poor compared with the resolution of PbWO₄ crystals (energy resolution better than 3% at room temperature) for all reasonably high energies. For lower magnetic fields as in, e.g., PHE-NIX, the forward tracking resolution would be even lower (gas detector type resolution is ~ 70 μm vs. while that of silicon is ~ 20 μm). The energy resolution of PbWO₄ can be further improved by cooling the crystals. Resolutions of better than 2% have been achieved at PANDA. For comparison, the energy resolution of lead glass is 5-6%. The best detector resolution at small angles, where the tracking resolution is poor, would thus be achieved by a high-resolution crystal inner part. In general, the resolution of the calorimeter out to a critical distance r_0 and a critical angle θ_0 is given by the sum of the resolution at r_0 and the shower width. PbWO₄ has the smallest Moliere radius of all scintillating crystals and is thus the optimal choice. Determining r_0 and θ_0 is part of ongoing studies.

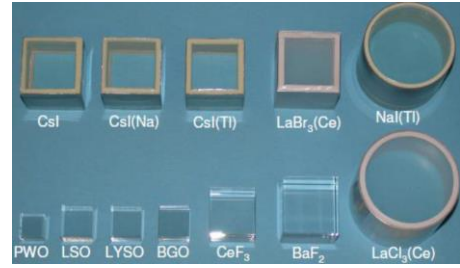
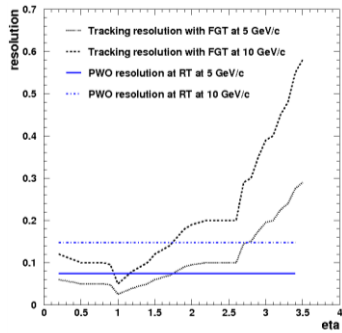


Figure 5: (left) Tracking resolution as function of angle for two representative momenta needed for the experiments for two different momenta (5 GeV/c and 10 GeV/c); (right) Various crystals showing size for roughly $(1.5 X_0)^3$ of each type demonstrating that PWO has the smallest shower containment volume of any crystal.

Parameter	Unit	CMS PWO-I	PANDA PWO-II	EIC
Luminescence maximum	nm	420	420	420
Expected energy range of EMC	GeV	0.15-1000	0.01-10	0.1-15
Light Yield at RT	phe/MeV	≥ 8.0	≥ 16.0	$\geq 15?$
EMC operating temperature	$^{\circ}\text{C}$	+18	-25	
Energy resolution at 1 GeV	%	3.4	2.0	few $\%/\sqrt{E}$
LY(100ns)/LY(1us)		≥ 0.9	≥ 0.9	
Optical transmission at 360 nm	%	≥ 25	≥ 35	
Optical transmission at 420 nm	%	≥ 55	≥ 60	
Optical transmission at 620 nm	%	≥ 65	≥ 70	
Homogeneity at T=50%	nm	≤ 3.0	≤ 3.0	
Induced absorption coefficient Δk at RT, >100 Gy/hr	m^{-1}	≤ 1.6	≤ 1.1	$\leq 1.5?$
Mean value of Δk	m^{-1}		<0.75	

Table 1: Physical goals and crystal specifications from CMS and PANDA. The projected specifications for EIC are based on the former two.

Table 1 lists the physical goals and specifications for the PWO crystals for CMS and PANDA, which were used in earlier contracts with BTCP and crystals grown according to the Czochralsky technology. The stricter requirements of PANDA resulted in the development of the ‘‘PWO-II’’ crystals, which featured a 60% lower La and Y doping concentration level compared to ‘‘PWO-I’’ and an increase of a factor or two in light yield. A few initial estimates of ranges for the EIC are shown in the last column. The EIC requirement on radiation hardness may be lower than that of PANDA, but detailed studies have yet to be done. However, as shown in Figure 6, even a relaxed requirement on radiation hardness may be difficult to achieve in the current SIC production. This emphasizes the importance of our R&D efforts to develop an alternate supplier with Crytur. The general question whether the EIC could use more relaxed crystal specs, also in terms of variations, is a key question of our ongoing R&D.

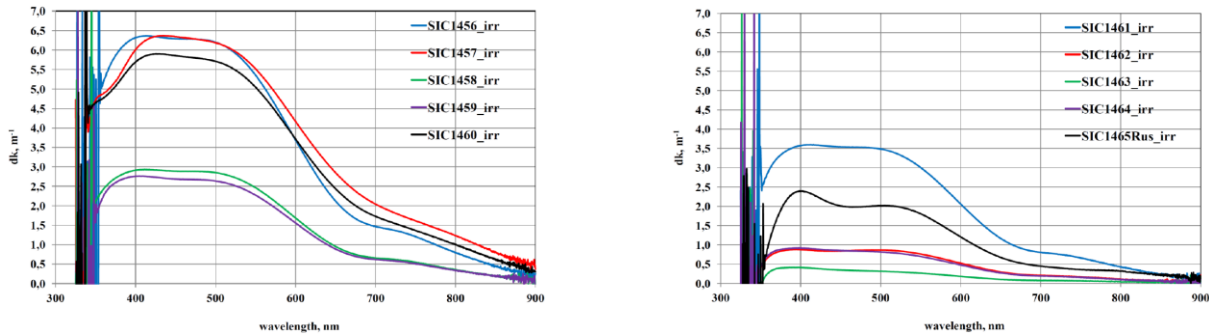


Figure 6: Impact of radiation damage in terms of the optical absorption coefficient for 10 PWO crystals from SIC produced in the fall of 2014. The data show very large fluctuations in radiation hardness. Only three out of ten crystals would pass the requirements listed in Table 1.

Assuming that our first year PbWO₄ crystal studies continue successfully, we are planning to build a small prototype detector consisting of a 5x5 matrix of the new improved crystals in the second year of our R&D. This would allow us to study these crystals in test beam and measure the actual energy and position resolution that we could achieve with them. This beam test would most likely be done at either SLAC where one can obtain a high precision beam of electrons with a momentum up to 15 GeV or at Jefferson Lab where the upgraded CEBAF provides electron beams up to 11 GeV.

The prototype setup could be based on that for the JLab NPS, which has an active area of about 6x6 cm² including a crystal matrix of PbWO₄ (and PbF₂ to test hybrid configurations of crystals) in a copper frame. The readout is done by 19 mm Hamamatsu R4125 PMTs with a JLab developed new active HV base. The prototype will test light monitoring as well as two approaches for a crystal curing system: a standard system with a blue light source and IR curing with wavelengths > 900 nm. The NPS prototype IR curing system was constructed using superbright LEDs like the OSRAM LD274 with a peak wavelength of 950 nm and Vishay TSAL7400 with a peak wavelength of 940 nm. One could consider using the NPS prototype or a modified version of it, which could provide flexibility in the construction schedule.

As a second stage of testing we propose to investigate reading out the calorimeter with SiPMs or other sensors with tolerance to radiation and magnetic fields. This would be the first time SiPMs would be used to read out this type of calorimeter. We will benefit from JLab's experience with these devices with, e.g., the GluEx project and the DIRC project, which is also funded by the EIC R&D program. We expect that we will be able to reuse many of the SiPMs from our R&D on the barrel calorimeter, and therefore will not need to purchase new SiPMs for this test. We should also be able to use much of the readout electronics and the calibration system from the small tungsten scintillator prototype calorimeter that was built as a part of that project. Most other electronics, such as amplifiers, discriminators, scalers, readout controller and DAQ, system are available at JLAB. Therefore, the main item that would need to be purchased for constructing the PbWO₄ prototype calorimeter would be the actual crystals for the matrix.

What are critical issues?

At this stage, the most critical issues are to have finalized setting up the infrastructure for crystal testing, e.g., at IPNO, and to complete the procurement of the full-size crystals from Crytur.

Additional information:

The funds requested for our second year R&D in FY16 can be found in Section 6 of our FY15 proposal and amounts to \$120K. We will be requesting these funds at the next meeting of the Advisory Committee.

Sub Project: R&D on a Forward BSO Crystal Calorimeter for EIC

Project Leader: Y. Zhang

What was planned for this period? What was not achieved, why not, and what will be done to correct?

1) Some progress on BSO crystal production (from SICCAS):

a) Improved the temperature uniformity and stability control during the material melting and sintering. Fig. 1 left panel shows an example of the temperature controlled as a function of material height in the crucible.

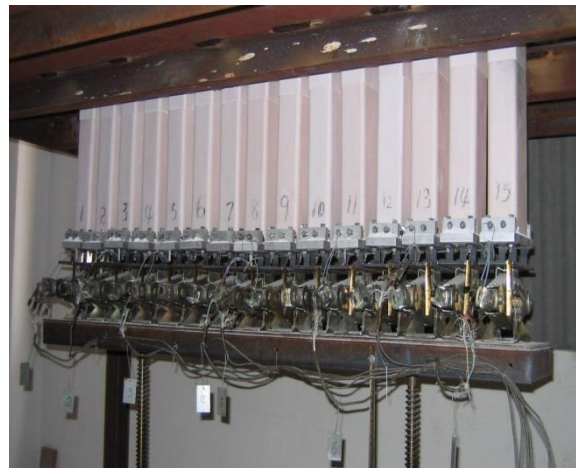
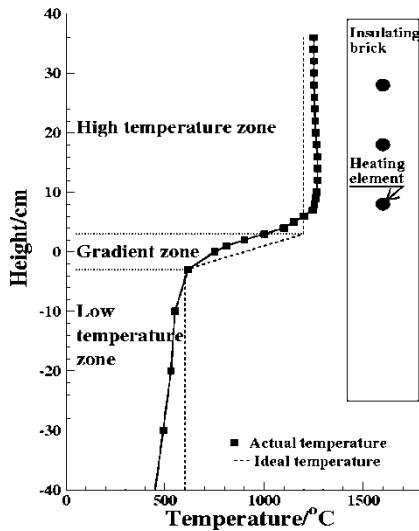


Fig. 1: Left: Temperature as a function of material height. Right: Production array with multiple crucibles

b) Enlarged the cross-section size of crucible, improved the purity and the transmittance, which makes larger-sized BSO crystals possible.

Fig. 2 shows the picture for a raw ϕ -55x120 mm BSO crystal without polishing.



Fig.2: Raw BSO crystal with ϕ -55x120 mm.

c) Potential mass production is promising. The current production system allows 30 crystals growth in parallel. It can be extended according to the demands.

2) Progress on simulation:

We continue the simulation on the BSO crystal performance with 3x3, 5x5 and 9x9 modules in Geant4. Fig. 3 shows an example of electromagnetic shower display in the 3x3 BSO crystal modules. The energy leak, <8%, for 3x3 module is a good reference for our estimate on the prototype calibration. The energy resolution and energy linearity, as a function of incident energy and incident angle are simulated, shown in Fig.4 and Fig.5.

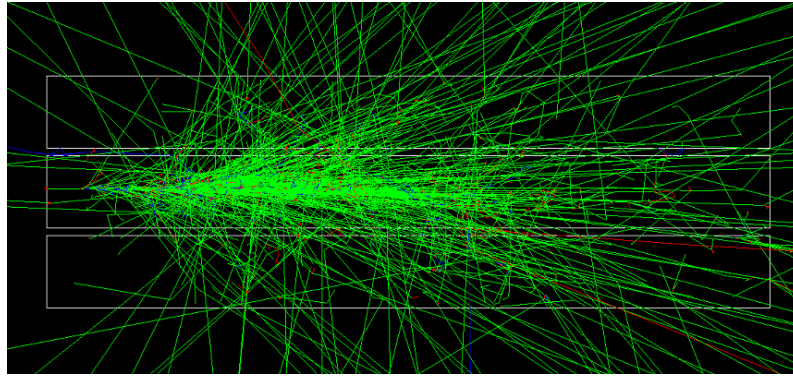


Fig.3: EM cascade shower in the 3x3 BSO crystal module.

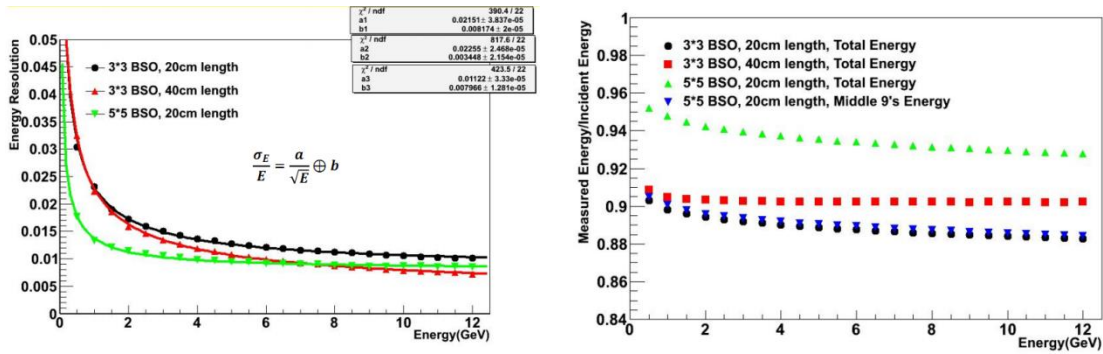


Fig. 4: Energy resolution and linearity as a function of incident energy.

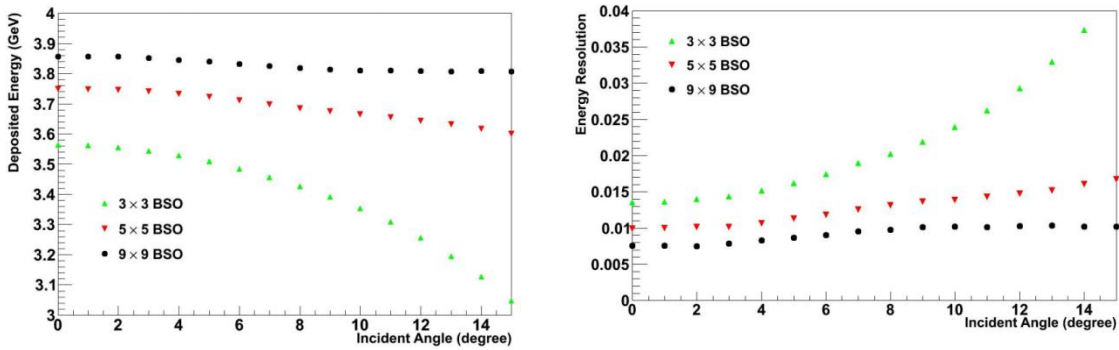


Fig.5: Deposit energy and energy resolution as a function of incident angle.

Due to the dependence of the incident angle, we are trying to design the module with two options: a) with placing the rectangular crystals according to the pseudo-rapidity in the forward direction; b) with trapezoid shape of the crystals. This work is ongoing.

3) Test the prototype with completely assembled 3x3 crystals before the beam test.

3.1) Module mapping.

Because of geometric symmetry, the energy deposit in symmetrical place is expected to be the same. Thus the crystals in the array are numbered as place 1, 2, 3.

#	BSO	1	2	3	4	0	6	7	8	1
	LY[p e/MeV]	7.9	3.9	9.8	6.9	3.9	8.4	3.5	6.9	1.2
#	PMT	829	847	848	833	832	845	830	843	844
	Gain HV= -800V	.6e5	.1e5	.3e5	.7e5	.6e5	.2e5	.7e5	.4e5	.9e5

Table 3: Mapping of crystal number and PMT parameters.

3.2) Module dynamic determination for calibration and beam test.

Since most of the energy is deposit in the centroid crystal (CH4) and less energy spread in the nearby crystals, we have to treat the center and surrounding area differently, see Section 3.1 and Table 1.

a) In the center channel, CH4, due to large amount of energy deposit, to avoid PMT reaching dynamic range limit, we have to determine lower HV.

b) In the four corners, CH0, 2,6,8, we have to determine the HV threshold to obtain enough photoelectrons due to small amount of energy deposit.

c) Another potential issue is related to the calibration. For the upcoming beam test, the energy of electron beams used to for calibration is $> 1\text{GeV}$. If the HVs are set too high, PMTs in place 2 and place 3 will reach to dynamic range limit.

From previous study, we know the $\text{Gain}=1.25\text{e}5$, $\text{DY} = 1300\text{pc}$. Both cathode and anode linearity characteristics only depend on the current value if the supply voltage is constant (from Sect. 4.3.2 of HUMMUTUSU Handbook), so we assume the dynamic range will be the same if the gain in each PMTs are the same.

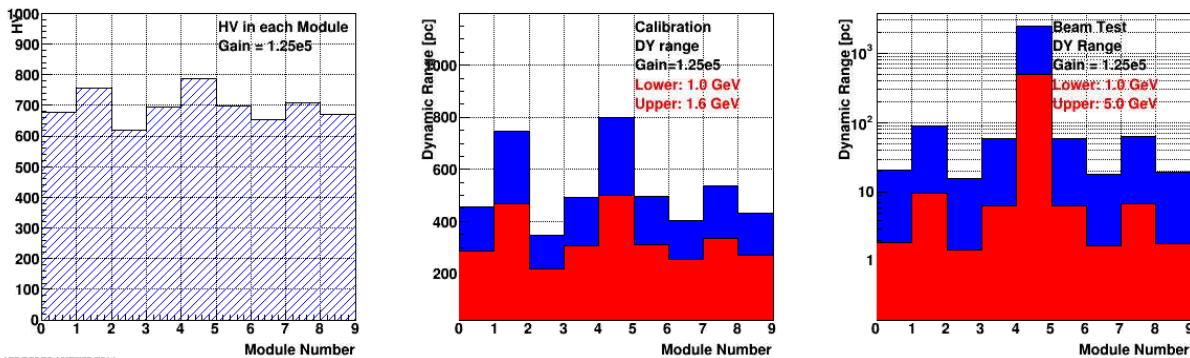


Fig.8: Dynamic range and HV in each channel with Gain = 1.25e5.

Figure 8 left panel shows the HV applied according to the module number to keep the uniform Gain = 1.25e5. Middle panel shows the collected charge distributions in each channel when electron inject at the middle of each module. The deposit energy is from simulation. The red and blue bars represent the dynamic range for each module with 1.0 and 1.6 GeV incident energy, respectively. This estimation is for calibration purpose. Right panel shows the same estimation but for measurement of energy resolution in the beam test. The deposit energy is from simulation. The red and blue bars represent the dynamic range for each module with 1.0 and 5.0 GeV incident energy, respectively.

Figure 9 tells us with uniform Gain= $1.25e5$ for each channel, the collected charge in place 2 and place 3 are under control, but place 1 hits the dynamic range limit.

To solve this issue we can reduce the HV in place 1. However, if the HV is too low, the PMTs cannot work properly.

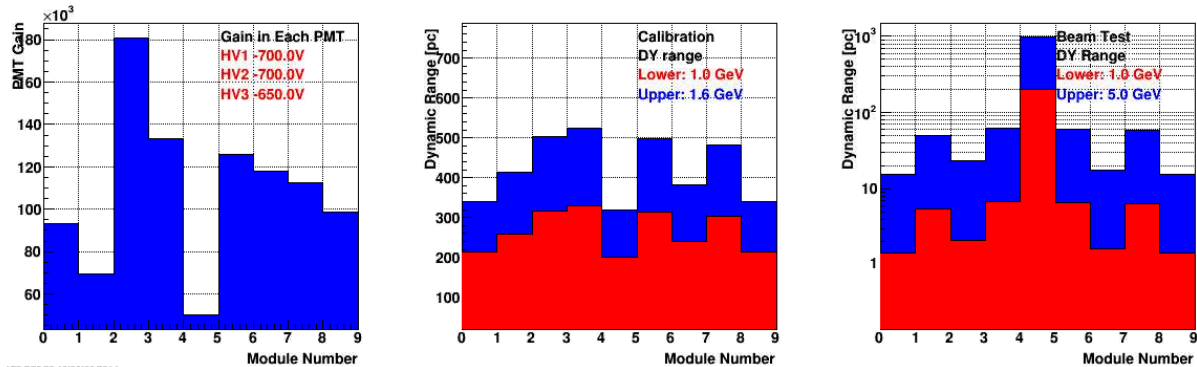


Fig.9: Dynamic range with tuned HV in three HV channels.

Reduce HV1 to -700V. The Gain in module 4 drops to $5e4$, the collected charge will reach to 1000pc (very close to current PMT dynamic range but safe). The signal for each channel can be clearly seen with HV = -700V, -700V and -650V for three HV channels during the cosmic ray test, see Fig.11.

3.2) Test system at BNL

Figure 10 shows the test system at BNL (photo taken by Long Zhou). We do not have DAQ so far for this pre-test. However, this is enough for the signal check in each channel and some estimation (see next section). Hank Crawford from LBNL promised to provide us his DAQ boards during the beam test. If possible we will try cosmic ray test with this DAQ system at BNL.

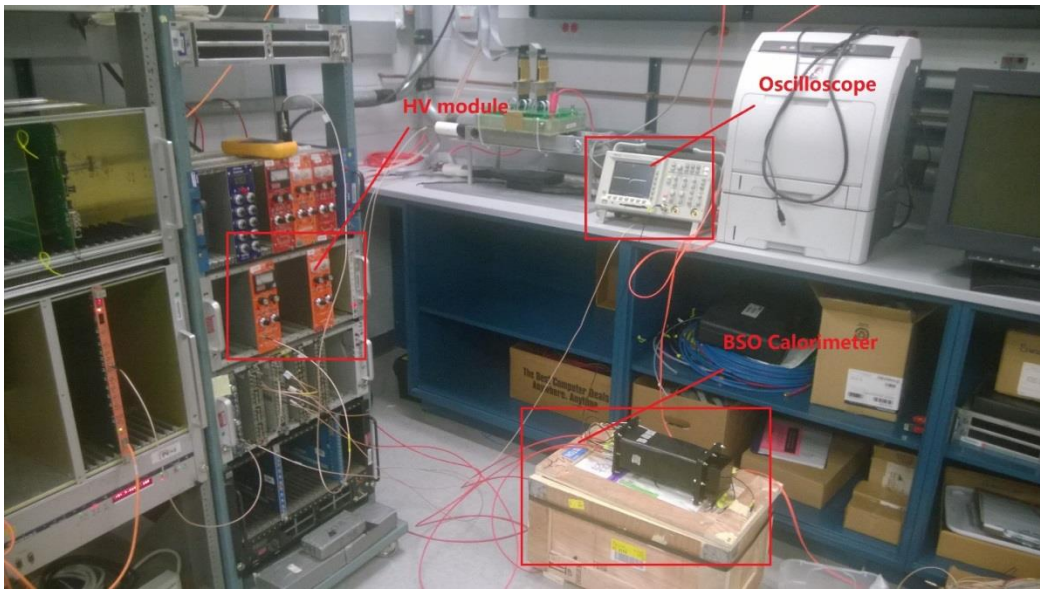


Fig. 10: Test system without DAQ

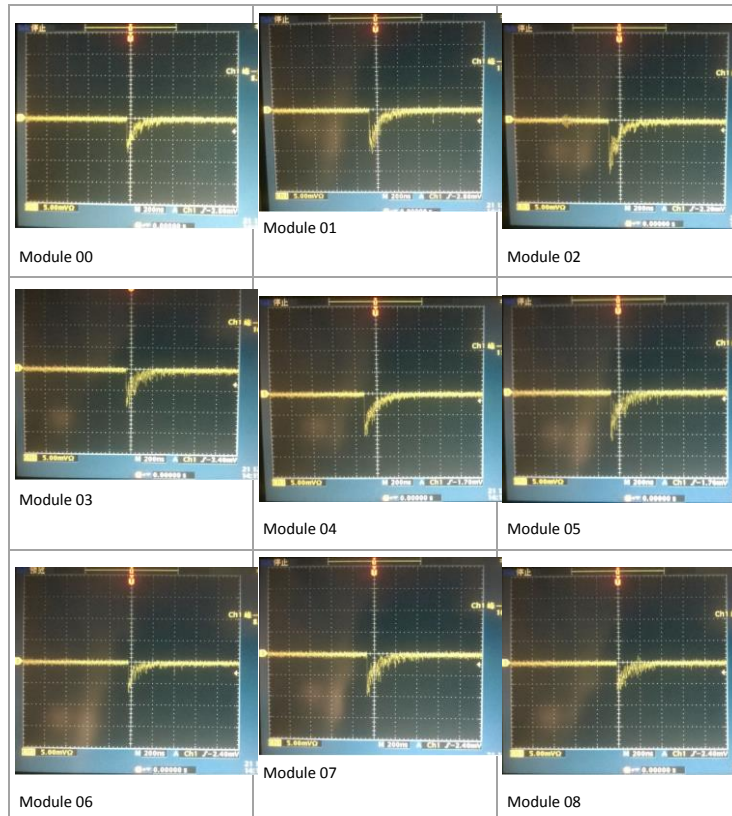


Fig. 11: Signal in each channel in cosmic ray test.

The signals in 9 channels are observed normally in the cosmic ray test, shown in Fig. 11.

What was not achieved, why not, and what will be done to correct?

The original plan for the beam test was around November 2014 at CERN together with the DAMPE group. We changed the plan because 1) there could not be enough beam time for us if we work with DAMPE group, 2) there will be a beam test at SLAC as well around December 2014 with a STAR HCal prototype test arranged by Hank Crawford and he kindly can provide us the DAQ boards. We delivered the BSO prototype to BNL around November 10th, 2014. However, the beam test was delayed due to the changes of SLAC beam schedule. The next opportunity will be around end of January, 2015.

Future

- 1) Finish the beam test and summarize the test results compared to simulation.
- 2) Continue simulation study on the BSO based calorimeter performance with new geometry design.
- 3) Continue working with SICCAS, probably will have more BSO crystals for testing (larger size, better performance). The crystal growth cost will be covered by their own funds. In addition, it is expected that a collaboration from the high energy physics community (ANL, Caltech and Fermilab) working on developing a homogenous hadronic calorimeter (HHCAL) will provide supplemental funding for this effort.

Sub Project: Simulations on calorimetry and related systems for an EIC detector

Project Leader: E.C. Aschenauer

Past

What was planned for this period?

- To tune the February'2014 T1018 FNAL test run geometry in the Monte-Carlo (including dead material) and GEANT physics lists in the simulation in order to reproduce better the measured data.
- To crosscheck the requirements for backward electromagnetic calorimeter energy resolution based on physics needs in terms of lepton/hadron separation.

What was achieved?

For the recent February'2014 T1018 test run a combined EmCal+HCal geometry (see picture below) was carefully (re)modeled.

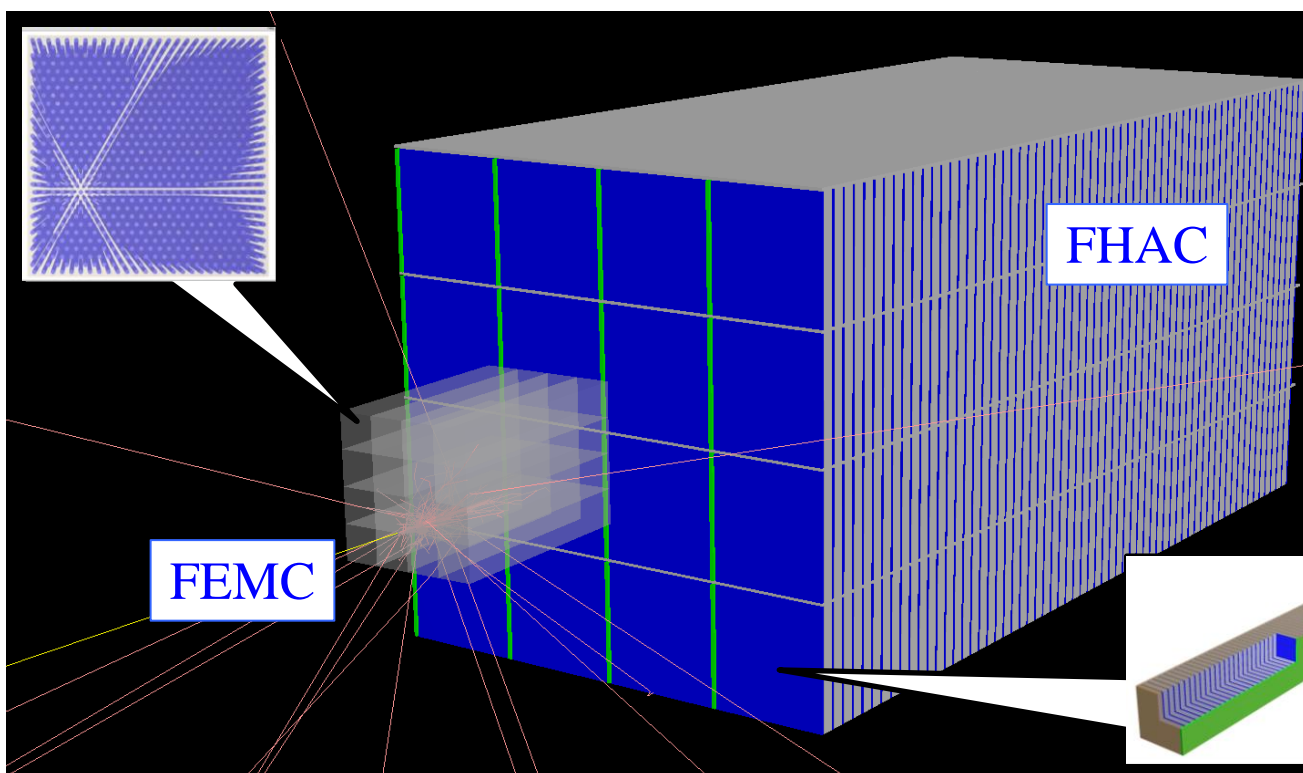


Figure-1: Electromagnetic and hadronic calorimeters of the February'2014 T1018 test run setup (4x4 tower arrangement). Internal details of calorimeter towers are shown in captions.

Internal structure of both electromagnetic (tungsten powder scintillating fiber) and hadronic (lead plate scintillating plate) sampling calorimeters is now described to as much detail as needed for conclusive comparison between data measured in the test run and the simulation results. For the former (spaghetti) calorimeter type this includes precise description of fibers themselves (material; core and cladding dimensions), fiber matrix arrangement inside a given elementary calorimeter cell (tower), absorber material composition and brass meshes. For the latter (sandwich) calorimeter type the 3D arrangement of scintillating plates, lead absorber, WLS as well as steel spacers and even steel assembly pins is modelled according to the design drawings. EmCal rotation by 4 degrees around

vertical axis as well as the presence of thick assembly steel plate in front of HCal in the test run setup (not shown in the figure) were accounted as well.

We switched to FTFP_BERT physics list usage in the GEANT4 simulation and accounted Birk's correction for polystyrene by hand in digitization phase. This allowed eliminating a noticeable discrepancy between lepton and hadron signal spectra between measured data and the Monte-Carlo. The correlation between energy response in EmCal and HCal sections for hadrons (see picture below) looks now almost identical to the measured data (compare to fig. 1.6 in July'2014 report).

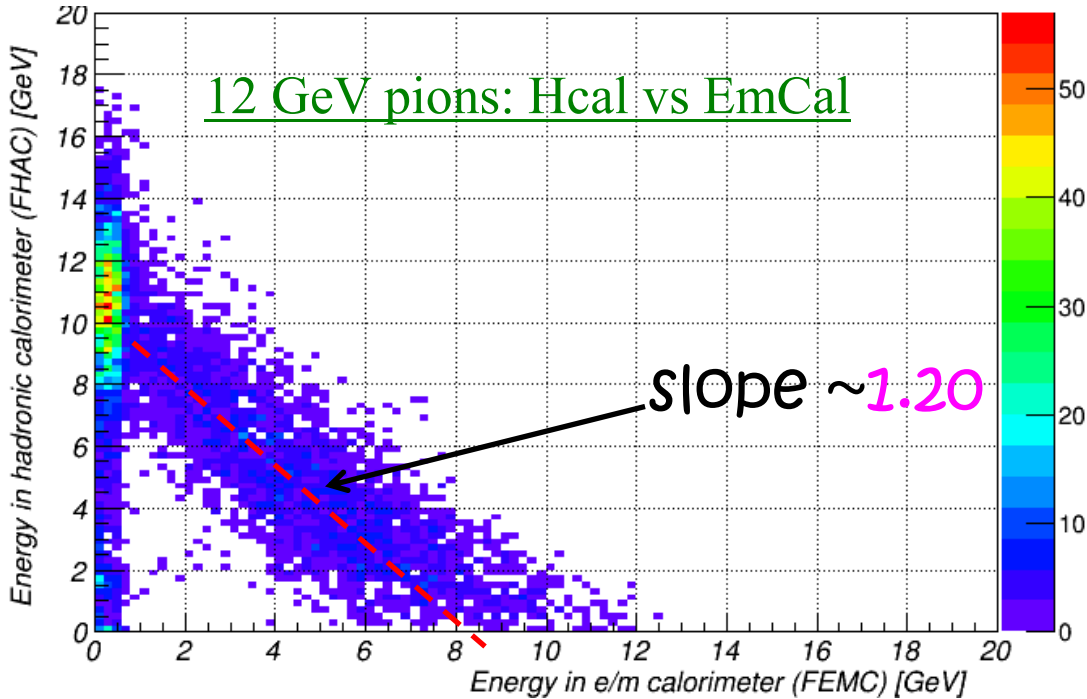


Figure-2: Simulated energy response correlation between electromagnetic and hadronic calorimeters of the February'2014 T1018 test run setup.

Simulated results on linearity in HCal+EmCal combined signal, as well as energy resolution on hadrons basically match the expectations from measured data (compare also to Fig. 1.8 in July'2014 report).

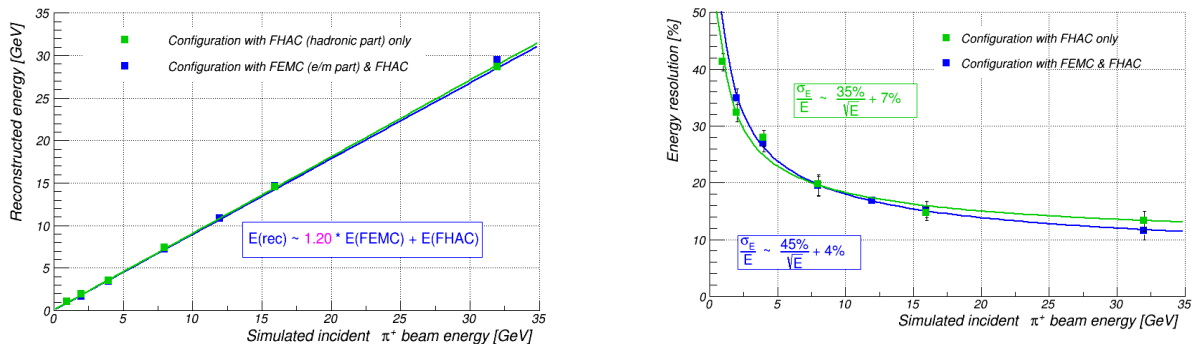


Figure-3: Left panel: response linearity of HCal+EmCal system with incident hadron energy, up to 32 GeV. Right panel: energy resolution of order of $\sim 40\text{-}45\%/\sqrt{E}$ is expected for this configuration.

It was demonstrated recently with the help of eic-smear code, that in electron-going direction one can maintain reasonably good lepton-hadron separation using electromagnetic calorimeter with a relatively moderate energy resolution, of order of $\sim 6\text{-}7\%/\sqrt{E}$, see pictures below.

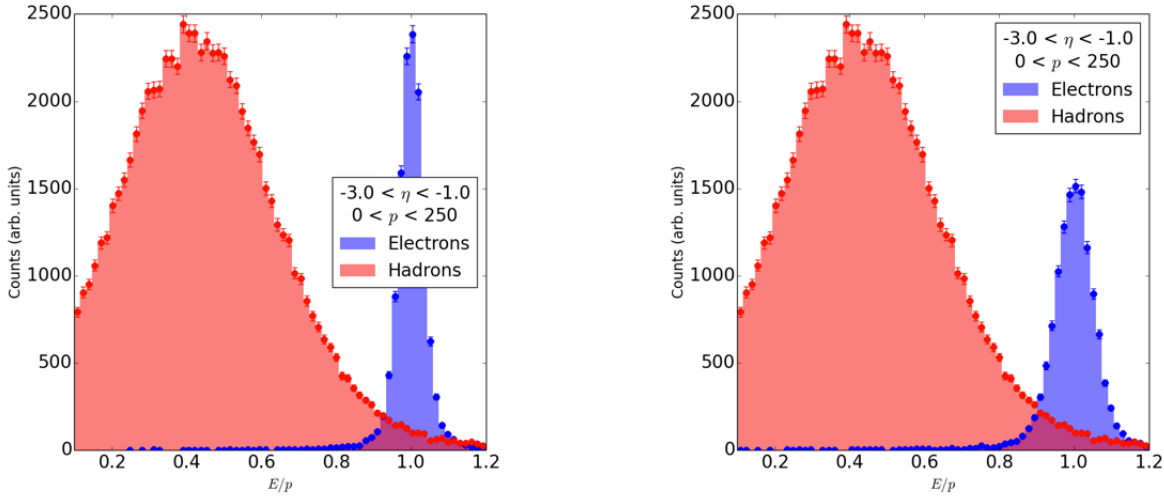


Figure-4: Left panel: lepton-hadron separation in lepton-going direction using lead glass crystal calorimeter with energy resolution $\sim 6\%/\sqrt{E} + 0.8\%$ (PHENIX working setup). Right panel: the same, using sampling calorimeter with $\sim 10\%/\sqrt{E} + 1.5\%$.

Therefore (at least for pseudo-rapidity range of $[-3 \dots -1]$ or so) one can possibly replace expensive PWO crystal electromagnetic calorimeter in the default EIC model detector setup by the metal powder scintillating fiber one, provided energy resolution for this technology is pushed to its limits. Natural options are to use thinner fibers in configuration with a smaller fiber-to-fiber distance (increase sampling frequency) and/or to use absorber with smaller density (increase sampling fraction). Plots below demonstrate that in otherwise “ideal” configuration using 400-micron fibers and absorber with tin powder admixture one can possibly attain the required level of resolutions.

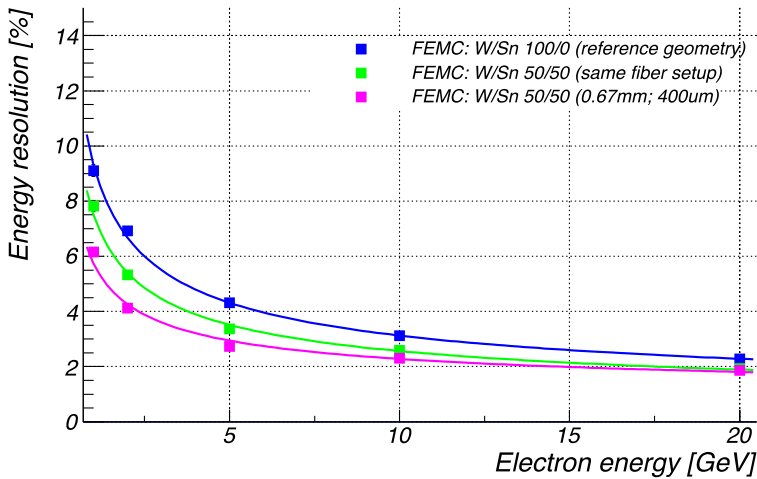


Figure-5: Simulated energy resolution of tungsten (or tungsten+tin) powder scintillating fiber calorimeter for various combinations of fiber diameter, fiber-to-fiber distance and absorber composition. Example configuration with 400 micron fibers, 670 micron mesh honeycomb parameter and absorber with metal powder Sn/W in composition 50/50 by weight (rather than with pure tungsten used so far) gives in ideal case $< 6\%/\sqrt{E}$ energy resolution with a constant term $< 1\%$ (magenta curve).

Future

What is planned for the next funding cycle and beyond? How, if at all, is this planning different from the original plan? We plan to optimize the geometry of tungsten+tin powder scintillating fiber calorimeter with 400 micron fibers in order to attain as high energy resolution as this technology allows.

Additional Information:

In its report from last July, the Committee commented that not enough progress had been reported on simulations for both detector design and physics to develop detector requirement specifications and physics capabilities for a comprehensive detector at EIC. In fact, a great deal of simulation results in these areas had already been produced at that time, but perhaps they were not presented clearly enough to the Committee. However, now many of those results have been summarized and are presented in the eRHIC Design Study that is now available on the web (<http://arxiv.org/pdf/1409.1633.pdf>). In particular, Chapter 4, “eRHIC Detector Requirements and Design Ideas” explicitly gives the set of detector requirements and physics capabilities for a dedicated EIC detector (BeAST), as well as for the upgraded detectors for PHENIX and STAR.